

The β to γ (insulator-metal) transition in BiFeO_3

Donna C. Arnold¹, Kevin S. Knight², Gustau Catalan³, Simon A.T. Redfern³, James F. Scott^{3,4}, Philip Lightfoot¹ and Finlay D. Morrison^{1*}

¹ *School of Chemistry, University of St Andrews, North Haugh, St Andrews, Fife,
KY16 9ST, UK*

² *ISIS Facility, Rutherford Appleton Laboratory, Chilton, Didcot, OX11 0QX, UK*

³ *Department of Earth Sciences, University of Cambridge, Downing Street,
Cambridge, CB2 3EQ, UK.*

⁴ *Department of Physics, University of Cambridge, J. J. Thomson Ave., Cambridge,
CB3 0HE, UK*

* *To whom correspondence should be addressed: e-mail: fm40@st-andrews.ac.uk,
Tel: +44-1334463855, Fax: +44-1334463805.*

Abstract

High temperature powder neutron diffraction experiments have been conducted around the reported β - γ , insulator-metal phase transition (~ 930 °C) in BiFeO_3 . The results demonstrate that while a small volume contraction is observed at the transition temperature, consistent with an insulator-metal transition, both the β - and γ -phase of BiFeO_3 exhibit orthorhombic symmetry i.e. no further increase of symmetry occurs under the present experimental conditions, contrary to previous suggestions. Furthermore we observe the γ -orthorhombic phase to persist up to a temperature of approximately 950 °C before complete decomposition into $\text{Bi}_2\text{Fe}_4\text{O}_9$ (and liquid Bi_2O_3), which subsequently begins to decompose at approximately 960 °C.

Introduction

The drive to find novel materials for applications such as data storage, spintronics and microelectronic devices has lead to a resurgence in research into multiferroic materials.^[1,2] By far the most widely studied multiferroic material is BiFeO₃, due primarily to its high temperature magnetic and electric transition temperatures: ferroelectric $T_C \sim 810 - 830 \text{ }^\circ\text{C}$ ^[3,4] and antiferromagnetic $T_N \sim 350 - 370 \text{ }^\circ\text{C}$.^[5] In fact as a result of the topical nature and popularity of BiFeO₃ a comprehensive review article on the key research advances, encompassing ceramic, single crystal and thin film morphologies, has recently been reported.^[6]

Despite extensive studies on bulk BiFeO₃ there are still many contradictions in the literature. In particular the high temperature phases have been well studied, though are still not fully understood. In the early work as many as eight anomalies in physical properties as a function of temperature, based on electrical and magnetic measurements, have been reported.^[7,8] However, it is now more generally accepted that there are two main anomalies which coincide with the transitions at T_N and T_C . A third transition has been reported by some authors at a temperature of approximately $190 \text{ }^\circ\text{C}$.^[8] However, the nature of this transition has never been fully understood, with some authors reporting evidence for this transition in structural studies whilst others make no reference to it. Variable temperature X-ray powder diffraction (XRPD) studies^[9], suggested two anomalies in lattice parameters at T_N and T_C and this was later supported by a powder neutron diffraction (PND) study.^[10,11] These authors reported the evolution of the rhombohedral (R3c) α -phase up to a temperature of $700 \text{ }^\circ\text{C}$ before significant decomposition to Bi₂Fe₄O₉ occurred; a problem which occurs in many studies of BiFeO₃ at elevated temperatures.

More recently an updated phase diagram for BiFeO_3 ^[12] has been reported based on thermal analysis, spectroscopic, diffraction and other methods. This work suggests evidence of three distinct solid phases above room temperature and below the melting point ($\sim 960^\circ\text{C}$): the rhombohedral α -phase, below T_C , an intermediate β -phase, in the region $830 - 925^\circ\text{C}$, and a cubic γ -phase in the region $925 - 933^\circ\text{C}$ before decomposition and subsequent melting. Many symmetries for the β - BiFeO_3 phase have been suggested by x-ray diffraction and first principle techniques including tetragonal (space group $I4/mcm$),^[13] monoclinic ($P2_1/m$),^[14] orthorhombic^[12,15] and rhombohedral ($R-3c$).^[16] Recently we demonstrated, by high resolution PND experiments, that the β -phase crystallises in the orthorhombic $Pbnm$ space group, the same as non-polar GdFeO_3 .^[15]

In contrast, little work has been reported for the β - γ phase transition, primarily due to the onset of decomposition before this temperature is reached.^[14,15] Palai *et al.* suggested the γ -phase adopts cubic symmetry, with this transition reported to coincide with a insulator-metal transition.^[12] This was supported by band structure models, high-temperature dc resistivity and light absorption and reflectivity measurements which show the band gap decreases with increasing temperature before dropping abruptly to zero at $\sim 930^\circ\text{C}$.^[12] More recently the presence of a metal-insulator transition has been reported using ab-initio calculations^[17] and in high pressure^[18,19] and spectroscopic ellipsometry studies.^[20,21]

Here we present high temperature powder neutron diffraction data in the temperature range 900°C to 960°C . Through careful design of the experimental set-up and the collection of short data runs (~ 5 mins) we have been able to minimise the onset and subsequent rate of decomposition of BiFeO_3 into the parasitic $\text{Bi}_2\text{Fe}_4\text{O}_9$

phase. We report a subtle drop in the cell volume at approximately 930 °C consistent with the previously reported insulator-metal transition. However, in contrast with previous reports we demonstrate that BiFeO₃ is in fact orthorhombic over the whole temperature range investigated. This has important consequences for our understanding of the origin of the metal-insulator transition.

Experimental

Single phase BiFeO₃ was prepared using the method previously described by us.^[15] Stoichiometric ratios of Fe₂O₃ (Aldrich, ≥ 99 %) and Bi₂O₃ (Aldrich, 99.9 %) were reacted with a 6 mol % excess of Bi₂O₃ at 800 °C for 5 hours. After calcination the material was ground into a fine powder and leached with 2.5 M nitric acid under continuous stirring for 2 hours, washed thoroughly with distilled water and dried at 400 °C for 1 hour. XRPD confirmed single phase BiFeO₃.

PND data were collected on the HRPD instrument at ISIS, over a temperature range of 900 °C to 960 °C. Short data collections (~5 mins) were undertaken when the furnace reached temperature, with a second run (~ 5 mins) collected immediately after the first. A third 5 minute run was also collected at 900 °C in order to allow the material to equilibrate at these elevated temperatures. Due to the high partial pressures in the system as a result of the high temperature decomposition of BiFeO₃ into Bi₂Fe₄O₉ and liquid Bi₂O₃ the experiment was conducted under flowing N₂. This was achieved by taking BiFeO₃ powder compacts which were suspended on a quartz frit within a quartz tube. The tube was then mounted within the furnace with the thermocouples attached to the top of sample material and N₂ flowed over the closed system.

For XRPD data collection polycrystalline ceramic BiFeO₃ was ground under acetone and mounted on an alumina sample holder within the MRI high-temperature chamber of a Bruker D8 Advance diffractometer. Data were collected in θ - 2θ geometry using CuK $_{\alpha}$ radiation, Göbel mirror parallel beam primary optics and Soller receiving slits with a Vantec position sensitive detector. Diffraction patterns were obtained in situ at high temperature by rapid scans over the region of interest (20° to 60° 2θ) such that the sample was held at each temperature for no more than five minutes, with temperature steps varying between 15 and 20 K.

Results and Discussion

Crystallographic analysis of PND data collected at 900 °C confirmed the formation of β -BiFeO₃. Interestingly, as a result of the fast heating rates and short scan times employed in order to minimise decomposition to Bi₂Fe₄O₉ and liquid Bi₂O₃, a small amount of the α -phase (i.e. R3c phase) was seen to persist for approximately 10 minutes at 900 °C before full transformation into the Pbnm β -phase. The data collected for the 3rd five minute run showed no evidence of any un-indexed peaks further confirming our previous assessment of the orthorhombic character of the β -phase.^[15] Rietveld refinement of these data was performed using the GSAS suite of programs^[22] with the refinements including individual isotropic atomic displacement parameters for all atoms as well as the usual profile coefficients. The refinement profile is given in figure 1 with further details given in table 1. With increasing temperature BiFeO₃ can be seen to decompose to Bi₂Fe₄O₉ (and liquid Bi₂O₃), with approximately 5 % of this phase observed at 910 °C, increasing rapidly to approximately 80 % at 950 °C despite the short scan times and high heating rates

employed. A reliable full refinement was also performed on the 2nd 945 °C data set as given in figure 1(b) and table 1. However at intermediary (and higher) temperatures, whilst all data were modelled using the Rietveld method, it was only possible to extract quantitatively the lattice parameters as a result of increasing amounts of 2nd phase and in the intermediary data the presence of shoulders on the main BiFeO₃ peaks (discussed below). A summary of the extracted parameters and relative phase percentages over the temperature range 910 to 950 °C can be found in supplementary data, table S1. The thermal evolution of the cell volume of the BiFeO₃ phase is shown in figure 2. Between 900 °C and 930 °C the cell volume continues to increase in agreement with the data collected previously by us (figure 2b).^[15] At 930 °C there is a small decrease in the cell volume ($\Delta V/V = 0.15\%$) away from the observed trend. This is likely to result from shortening of the Fe-O bonds as the phase becomes metallic which is consistent with the observed drop in cell parameters. These observations are also consistent with the optical observations and band gap calculations of Palai *et al.*^[12] who were the first to suggest an insulator-metal transition. This subtle change in volume has also been observed at the metal-insulator transition in other transition metal perovskite oxides such as NdNiO₃.^[23] It would also be expected that this transition would be accompanied by a straightening of the Fe-O-Fe bond angle. However, it was not possible to perform full refinements to obtain accurate atomic positions and hence bond angles over the whole temperature range due to the deterioration in the data quality due to the increased temperature and also the decreasing signal-to-noise as the BiFeO₃ phase decomposes.

Previous reports have suggested that the metallic phase (γ -phase) exhibits cubic, Pm-3m, symmetry.^[12] This orthorhombic-cubic transition has also been reported in high

pressure experiments on BiFeO_3 ^[18] and also in Mn-doped samples ($\text{BiFe}_{0.7}\text{Mn}_{0.3}\text{O}_3$) at ambient pressure, which exhibits an analogous R3c to Pbnm to Pm-3m series of phase transitions.^[24] However, the latter remains semiconducting throughout with no evidence of a metal-insulator transition. In fact in this material the transition from Pbnm to Pm-3m is marked by a sudden increase in cell volume as opposed to the volume shrinkage expected in an insulator-metal transition and observed in pure BiFeO_3 . Close inspection of our data provides no evidence for the existence of a cubic phase, with peak splittings and peaks which violate cubic symmetry remaining clearly evident right up to full decomposition and melting (figure 3). Considering the work of Howard and Stokes^[25] the most likely tilt arrangements for perovskites transforming from Pbnm (Glazer notation $a^-a^-b^+$) towards Pm-3m ($a^0a^0a^0$) symmetry would suggest a possible transition to either tetragonal, $P4/\text{mbm}$ ($a^0a^0c^+$) or orthorhombic, Imma ($a^0b^-b^-$) symmetry. As with the cubic symmetry the presence of peaks and peak splitting which violate tetragonal symmetry rule out the possibility of a transition to tetragonal, $P4/\text{mbm}$, symmetry. This is particularly evident in the d-spacing region $2.20 - 2.40 \text{ \AA}$, where two peaks are clearly apparent over the whole temperature range investigated; these would be required to be a single peak to satisfy either tetragonal or cubic symmetries (figure 3). The possibility of an orthorhombic, Pbnm, to orthorhombic, Imma, phase transition cannot be ruled out since both phases would result in the two peaks observed. However, the similar nature of these two symmetries and the quality of the data collected makes it impossible to effectively distinguish between these two space groups. Nonetheless these results clearly indicate that both sides of the metal-insulator phase transition exhibit orthorhombic symmetry, such that either both the insulating and the metallic phase exhibit Pbnm symmetry or possibly a Pbnm to Imma phase transition occurs. These observations are remarkably similar in

nature to the case of orthorhombic RNiO_3 ($\text{R} = \text{Nd}$ or Pr)^[23], which exhibit metal-insulator (semiconductor) transitions which are not accompanied by a change of symmetry i.e. both phases exhibit Pbnm symmetry.

Further inspection of the data between 930 °C and 940 °C reveals the presence of shoulders on the main peaks of the Pbnm phase (figure 4), suggesting a possible region of phase co-existence either between the two orthorhombic phases or between the insulating and metallic phases, indicative of a first order phase transition. Again, this is remarkably similar to the RNiO_3 phase where the metal-insulator transition is first order in nature resulting in regions of phase co-existence.^[26] Above 945 °C these shoulders have disappeared, suggesting that full transformation of the phase has occurred, further confirming that both the β - and γ -phases exhibit orthorhombic character in contrast with previous reports.^[12,18] Attempts at multiphase refinements to model possible phase co-existence of an orthorhombic β -phase with either a cubic or tetragonal γ -phase were unsuccessful with both models failing to fit all shoulders present. The possibility of phase co-existence between two orthorhombic (Pbnm) phases with different lattice parameters was also modelled. Figure 4 clearly shows excellent fitting of the shoulders further supporting the suggestion that these shoulders arise as a result of a first order transition between two orthorhombic (Pbnm) phases. The lattice parameters associated with this second phase, however, are fractionally lower than the β -phase (table 2) most likely as a result of the data quality and difficulties resolving exact shoulder positions. On a cautionary note, whilst the evidence supports a first order transition between two phases exhibiting orthorhombic symmetry, it should be stated the possible co-existence of alternative phases can not be completely ruled out. The γ -phase then persists up to temperatures of

approximately 955 °C before complete decomposition occurs. At this temperature (and above) the $\text{Bi}_2\text{Fe}_4\text{O}_9$ phase also begins to decompose into Fe_2O_3 and liquid Bi_2O_3 consistent with both the phase diagram and previous observations.^[12,14]

In an attempt to reconcile these observations with the previously reported cubic phase^[12,18] we modelled the two symmetries (i.e. orthorhombic Pbnm and cubic Pm-3m) as x-ray diffraction patterns with peak profiles estimated from our previous XRPD data using the CrystalDiffract[™] software^[27]. Comparison of the predicted x-ray diffraction patterns are shown in figure 5 and clearly indicate the similarities between the two symmetries. In particular the FWHM of the reflection corresponding to orthorhombic (200)/(112)/(020) and cubic (110) peak is insufficiently narrow to allow resolution of any splitting and hence differentiation between orthorhombic and cubic symmetries. In fact only subtle differences can be observed in the form of weak superlattice reflections in the orthorhombic symmetry which are absent in the cubic symmetry. We have repeated our refinements of the XRPD data in light of the neutron results discussed above and these show adequate fits using the Pbnm model (figure 6). Furthermore extraction of the lattice parameters over the temperature range studied with XRPD showed excellent correlation with those extracted from the neutron data (see supplementary data, figure S1). This would suggest that the ‘apparent’ loss of the orthorhombic superlattice reflections with increasing temperature which we previously assigned as an orthorhombic-cubic phase transition occur as a result of the loss of instrument sensitivity. These results highlight the limitations of laboratory-based x-ray diffraction studies for accurate phase identification in BiFeO_3 and emphasise the need for high resolution neutron experiments. Figure 7 shows the

evolution of lattice parameters as a function of temperature as obtained from PND data, which conclusively show the orthorhombic nature of both β - and γ -phases.

In addition to the conclusions that can be made directly from neutron scattering experiments, the domain wall structures in BiFeO_3 can be used to infer further information regarding structure and symmetry. J.-C. Toledano first demonstrated in 1974^[28] that it is necessary and sufficient for ferroelastic phase transitions that the crystal undergo a change in crystal class (trigonal-hexagonal is regarded as a single super-class in this argument). Thus, rhombohedral-rhombohedral transitions, as in LiNbO_3 , cannot be ferroelastic, nor can orthorhombic-orthorhombic transitions, as in KTiOPO_4 . Ferroelectric but non-ferroelastic transitions can exhibit only 180° domains in the lower-symmetry phase. In BiFeO_3 , however, the β -phase exhibits marked orthorhombic domains with walls that are NOT 180° : there are strong $(110)_{\text{pc}}$ walls ["pc" designates pseudo-cubic indexing], and weaker $(100)_{\text{pc}}$ walls intersecting them.^[12] These non- 180° walls therefore imply a higher-temperature phase (above the β -phase but not necessarily the γ -phase) that is not orthorhombic. This presents a paradox, since the present study shows clearly that the γ - β metal-insulator transition is orthorhombic-orthorhombic. The resolution of this paradox is that there may be an additional phase higher in temperature than the γ -phase. There is no evidence that this phase is thermodynamically stable. However, even thermodynamically inaccessible states can produce domains and domain walls: a good example is the family BaMF_4 ($M = \text{Co}, \text{Ni}, \text{Mg}, \text{Zn}, \text{Mn}, \text{Fe}$), all of which melt before their extrapolated $\text{mm}2$ to mmm transition is reached; yet all of them form from the melt in multi-domain structures.^[29]

More evidence for an ‘inaccessible’ cubic phase can be drawn from extrapolation of the pseudo-cubic lattice parameters of the orthorhombic β -phase. Such an extrapolation (figure 8) suggests that a and b parameters would converge at *ca.* 1020 °C, perhaps resulting in a tetragonal P4/mbm phase. Further extrapolation demonstrates that the lattice parameters converge to a single value above 1070 °C (figure 8); this would seem to support the existence of a high temperature transition to a non-orthorhombic (cubic, Pm-3m) symmetry. Such a sequence would follow the more widely observed sequence of transitions for perovskite oxides. While the extrapolation of data from the β -phase parameters should be viewed with caution, such a hypothesis is further supported by the Hamiltonians derived by Kornev *et al.* which predicted a transformation to cubic symmetry at a temperature of 1167 °C, well above the decomposition temperature.^[13] In reality the onset of metallic character in the γ -phase results in a shortening of the Fe-O bonds and a drop in unit cell volume, which disrupts the "natural" structural progression towards cubic symmetry.

These observed results also have important implications for the nature of the metal-insulator transition. Recently conflicting models for the metal-insulator transition, namely band-type^[12] and Mott-type,^[19] have been reported for BiFeO₃. Since a band-type insulator is required to have an even number of electrons in the unit cell (which fill the valence band completely such that there is a gap between them and the excited states in the conduction band) there has to be a structural transition whereby the number of formula units (and therefore the number of electrons) per unit cell changes in order for a valence band insulator to become a metal. On the other hand, in a Mott-type insulator the gap is due to electrostatic repulsion between the conduction electrons and therefore the transition from Mott-insulator to metal occurs when the

size of the electrostatic repulsion (the Mott-Hubbard parameter, U) is smaller than the width of the conduction band.^[30,31] Mott transitions are purely electronic and do not in theory require a change in either crystal structure or magnetic symmetry, although in practice the coupling between charge, spin and lattice means that other transitions tend to happen simultaneously.^[32]

Previously it was believed that the metal-insulator transition in BiFeO_3 was driven by the structural transformation from orthorhombic to cubic symmetry which leads to an enhancement in orbital overlap between the iron and oxygen ions.^[12,18] The data presented here clearly indicated that no structural transition occurs with both the β - and the γ -phases adopting orthorhombic symmetry. This would seem to rule out the possibility of a band-type model to describe the metal-insulator transition. It should also be noted that the possibility of a Pbnm to Imma phase transition could not be ruled out; however, both space group models exhibit identical unit cell parameters and therefore the same number of electrons which again rules against a band-type transition.

Gavriliuk *et al.* suggested a Mott-type transition, driven by a change in the spin state of the Fe^{3+} ion from high spin to low spin, in a pressure induced phase transitions,^[19] although it unlikely that such spin transition model is also valid for the temperature-driven transition. Pressure-induced high-spin to low-spin transitions with associated decreases in resistivity have also been reported in other perovskite orthoferrites,^[33,34] although the actual onset of the metallic state in these seems to take place at much higher pressures than the spin transition, indicating that the two are not necessarily correlated. On the other hand, the electron-electron repulsion energy U (the Mott-

Hubbard parameter) in the screened exchange model gives $E_g = 2.7$ eV in the ambient rhombohedral phase, and around 1.5 eV in the orthorhombic phase, but a negative -0.2 eV in the cubic phase.^[12,35] Since E_g is +1.5 eV in the orthorhombic phase and -0.2 eV in the cubic phase, it must reach exactly zero while still in the orthorhombic phase before turning cubic; at this point (semi)metallic conduction should set in, yielding an insulator-metal orthorhombic-orthorhombic transition without the need for a change in the spin configuration.

Catalan and Scott^[6] and, independently, Pisarev and co-workers^[20] have suggested that BiFeO₃ is a charge-transfer insulator with a band-gap controlled by the orbital overlap between the oxygen *p*- and the iron *d*-orbitals. The orbital overlap is heavily influenced by the Fe-O-Fe bond angle, θ : the straighter the angle, the bigger the overlap. Moreover, extrapolation of the temperature dependence of the bond angle and the optical bandgap in the rhombohedral phase indicates that a critical value $\theta_{MI}=159^\circ$ would be enough to drive the structure metallic, even in the absence of any symmetry change^[18]. Using the refinements of our 900 °C PND data we calculate Fe-O-Fe bond angles of $158.9(3)^\circ$ and $157.0(2)^\circ$ for the β -phase (semiconductor), while the 945 °C data yield Fe-O-Fe bond angles of $162(2)^\circ$ and $162(1)^\circ$ for the γ -phase (metal or semi-metal). Although there is some considerable error in the 945 °C data due to the dramatically reduced amount of perovskite BiFeO₃ phase and also the poorer signal to noise ratio there is good overall agreement with the thesis that the MI transition is driven by a critical straightening of the Fe-O-Fe angle (Figure 9).

Conclusions

In summary, we demonstrate that, in contrast with previous reports, both the β - and γ -phases exhibit orthorhombic symmetry either with no change in space group (Pbnm to Pbnm) or with a slight change in the octahedral tilt arrangement resulting in a transformation from Pbnm ($a^-a^+b^-$) to Imma ($a^0b^-b^-$). We also observe a subtle decrease in the unit cell dimensions during the transition which is consistent with the accompanying insulator-metal transition in BiFeO_3 . The β to γ transition is accompanied by a marked straightening of the Fe-O-Fe bond angle. This is consistent with the observed correlation between bond angle and optical bandgap, and suggests that the insulator-metal transition is due to a closing of the charge-transfer gap between the oxygen p orbitals and the iron d orbitals.

The absence of space group/symmetry change at a metal-insulator transition is not completely unheard of in perovskites and has previously been reported for both NdNiO_3 and PrNiO_3 , which are seen to exhibit orthorhombic Pbnm symmetry in both the metallic and insulating phases.^[23,26] In fact, these nickelates have been suggested to be fairly analogous to BiFeO_3 and have also been postulated to exhibit multiferroic character.^[26]

Acknowledgements

We thank the EPSRC, Royal Society and STFC for funding.

References

- [1] Y. Tokura, *Science* **2006**, 312, 1481
- [2] M. Bibes, A. Barthelemy, *Nature Materials* **2008**, 7, 425

- [3] Y. E. Roginskaya, Y. Y. Tomoshpolskii, Y. N. Venevstev, V. M. Petrov, G. S. Zhdanov, *Sov. Phys. - JETP* **1966**, 23, 47
- [4] W. Kaczmarek, Z. Pajak, *Solid St. Commun.* **1975**, 17, 807
- [5] G. A. Smolenskii, V. M. Yudin, *Sov. Phys. - Solid St.* **1965**, 6, 2936
- [6] G. Catalan, J. F. Scott, *Adv. Mater.* **2009**, 21, 2463
- [7] N. N. Kranik, N. P. Khuchua, V. V. Zhdanov, V. A. Evseev, *Sov. Phys. - Solid St.* **1966**, 8, 654
- [8] M. Polomska, W. Kaczmarek, Z. Pajak, *Phys. Stat. Solidi* **1974**, A23, 567
- [9] J. Bucci, B. K. Robertson, W. J. James, *J. Appl. Cryst.* **1972**, 5, 187
- [10] P. Fischer, M. Połomska, I. Sosnowska, M. Szymański, *J. Phys. C: Solid St. Phys.* **1980**, 13, 1931
- [11] A. Palewicz, R. Przeniosło, I. Sosnowska, A. W. Hewat, *Acta. Cryst.* **2007**, B63, 537
- [12] R. Palai, R. S. Katiyar, H. Schmid, P. Tissot, S. J. Clark, J. Robertson, S. A. T. Redfern, J. F. Scott, *Phys. Rev. B.* **2008**, 77, 014110
- [13] I. A. Kornev, S. Lisenko, R. Haumont, B. Dkhil, L. Bellaiche, *Phys. Rev. Lett.* **2007**, 99, 227603
- [14] R. Haumont, I. A. Kornev, S. Lisenko, L. Bellaiche, J. Kreisel, B. Dkhil, *Phys. Rev. B.* **2008**, 78, 134108
- [15] D. C. Arnold, K. S. Knight, F. D. Morrison, P. Lightfoot, *Phys. Rev. Lett.* **2009**, 102, 027602
- [16] S. M. Selbach, T. Tybell, M-A. Einarsrud, T. Grande, *Adv. Mater.* **2008**, 20, 3692
- [17] H.-J. Feng, F.-M. Liu, *Chin. Phys. Soc.* **2009**, 18, 1674

- [18] S. A. T. Redfern, J. N. Walsh, S. M. Clark, G. Catalan, J. F. Scott, <http://arxiv.org/ftp/arxiv/papers/0901/0901.3748.pdf> **2009**,
- [19] A. G. Gavriliuk, V. V. Struzhkin, I. S. Lyubutin, S. G. Ovchinnikov, M. Y. Hu, P. Chow, *Phys. Rev. B.* **2008**, 77, 155112
- [20] R. V. Pisarev, A. S. Moskvina, A. M. Kalashnikova, T. Rasing, *Phys. Rev. B.* **2009**, 79, 235128
- [21] O. E. González-Vázquez, J. Iñiguez, *Phys. Rev. B.* **2009**, 79, 064102
- [22] R. B. von Dreele, A. C. Larson, General Structure Analysis System (GSAS) (University of California, USA, 2001).
- [23] J. L. Garcia-Munoz, J. Rodriguez-Carvajal, P. Lacorre, J. B. Torrance, *Phys. Rev. B.* **1992**, 46, 4414
- [24] S. M. Selbach, T. Tybell, M-A. Einarsrud, T. Grande, *Phys. Rev. B.* **2009**, 79, 214113
- [25] C. J. Howard, H. T. Stokes, *Acta. Cryst.* **2005**, A61, 93
- [26] G. Catalan, *Phase Transitions* **2008**, 81, 729
- [27] D. Palmer, M. Conley, CrystalDiffract (Crystal Maker Software Ltd, Yarnton, Oxfordshire, 1994).
- [28] J.-C. Toledano, *Annals of Telecommunications* **1974**, 29, 249
- [29] J. F. Scott, *Rep. Prog. Phys.* **1979**, 42, 1055
- [30] N. F. Mott, *Rev. Mod. Phys.* **1968**, 40, 677
- [31] N. F. Mott, *Metal Insulator Transitions*. (Taylor and Francis, London, **1974**).
- [32] R. G. Moore, J. Zhang, V. B. Nascimento, R. Jin, J. Guo, G. T. Wang, Z. Fang, D. Mandrus, E. W. Plummer, *Science* **2007**, 318, 615
- [33] W. M. Xu, O. Naaman, G. Kh. Rozenberg, M. P. Pasternak, R. D. Taylor, *Phys. Rev. B.* **2001**, 64, 094411

- [34] G. Kh. Rozenberg, M. P. Pasternak, W. M. Xu, L. S. Dubrovinsky, S. Carlson, R. D. Taylor, *Europhys. Lett.* **2005**, *71*, 228
- [35] S. J. Clark, J. Robertson, *Appl. Phys. Lett.* **2007**, *90*, 132903
- [36] R. Przeniosło, A. Palewicz, M. Regulski, I. Sosnowska, R. M. Ibberson, K. S. Knight, *J. Phys. Condens. Matter* **2006**, *18*, 2069

List of Tables

Table 1: Structural parameters for β -BiFeO₃ at 900 °C, Space group Pbnm, a = 5.6298(1) Å, b = 5.6537(1) Å, c = 7.9861(2) Å and cell volume = 254.192(9) Å³. χ^2 = 0.9710, wRp = 7.78 %, Rp = 7.63 % and 945 °C, Space group Pbnm, a = 5.6311(2) Å, b = 5.6538(2) Å, c = 7.9885(3) Å and cell volume = 254.33(2) Å³. χ^2 = 1.029, wRp = 8.15 %, Rp = 7.87 %

Atom	Site	900 °C				945 °C			
		<i>x</i>	<i>y</i>	<i>z</i>	U(iso) x 100/Å ²	<i>x</i>	<i>y</i>	<i>z</i>	U(iso) x 100/Å ²
Bi	4c	0.9995(8)	0.015(1)	0.25	7.40(8)	0.999(3)	0.017(6)	0.25	12.4(5)
Fe	4a	0.5	0	0	1.86(4)	0.5	0	0	7.2(5)
O	4c	0.0631(7)	0.481(1)	0.25	4.7(1)	0.049(4)	0.470(7)	0.25	13(1)
O	8d	0.7105(6)	0.2896(6)	0.0318(4)	5.3(1)	0.7178(31)	0.278(4)	0.025(3)	15(1)

List of Figures

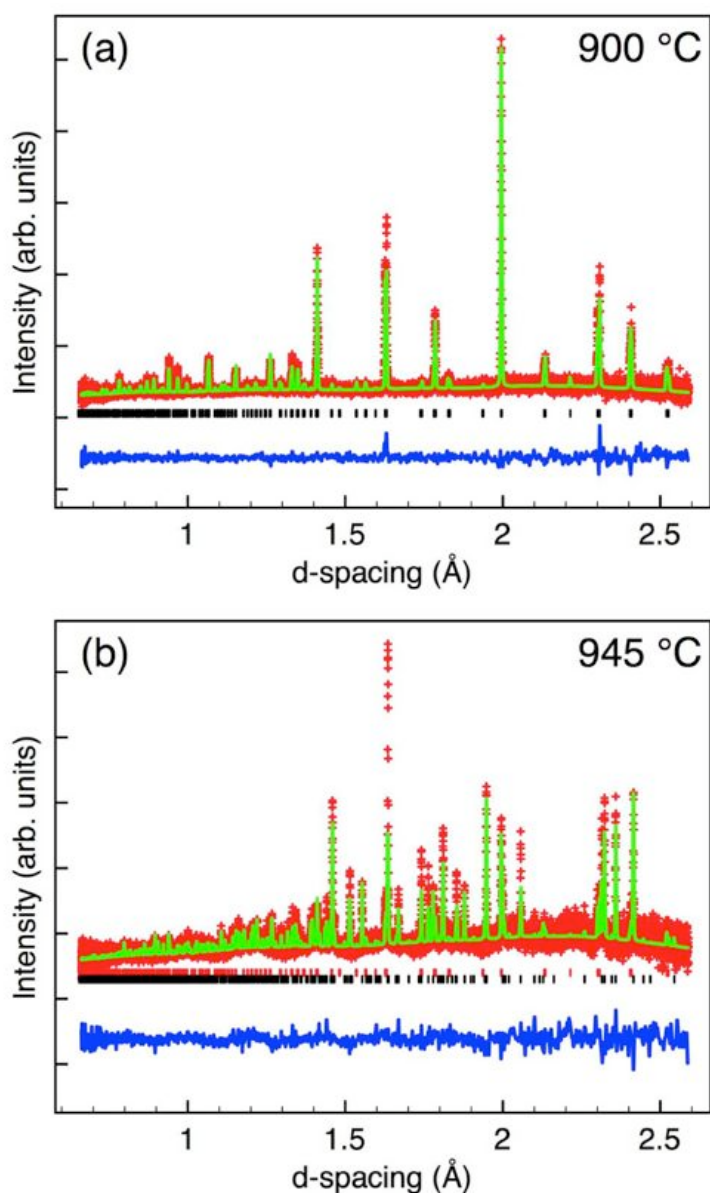


Figure 1: Refinement profiles at (a) 900 °C and (b) 945 °C showing the observed (+), fitted (solid line) and difference curves (bottom) for BiFeO_3 (both refined in the Pbnm space group) as represented by the bottom tick marks (top tick marks represent $\text{Bi}_2\text{Fe}_4\text{O}_9$). (Colour online).

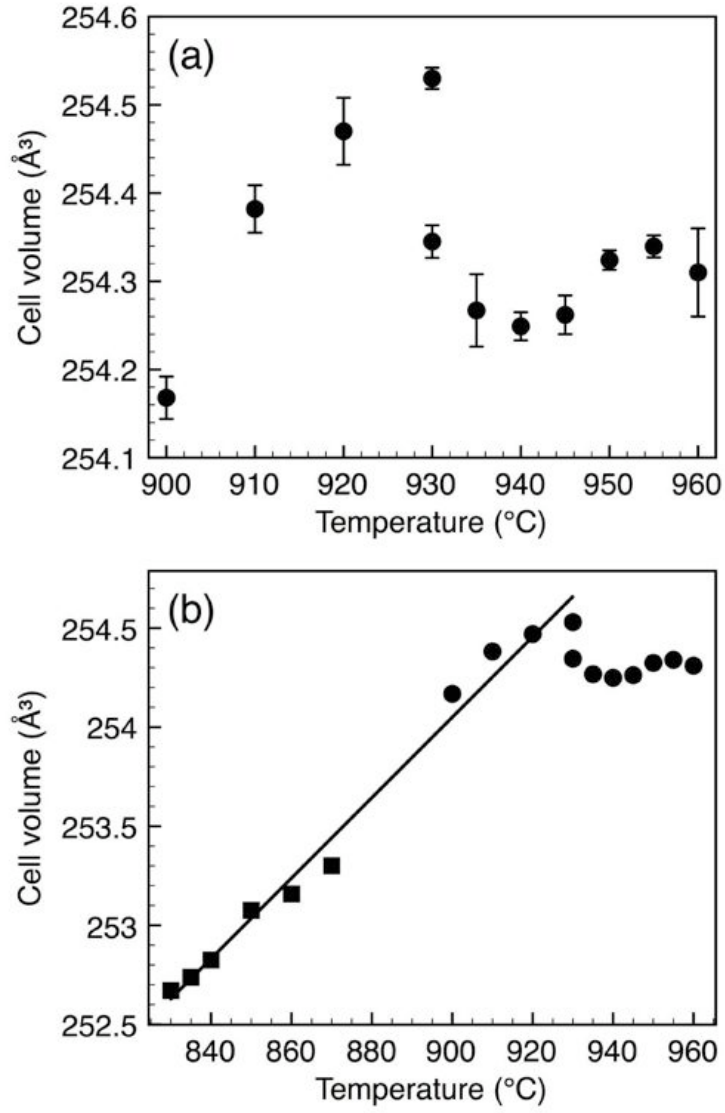


Figure 2: (a) Thermal evolution of the unit cell volume as a function of temperature in the $\beta\text{-BiFeO}_3$ phase. Error bars indicate differences between runs 1 (0-5 min) and 2 (5-10 min). (b) Extrapolation to include the data (■) collected in our previous experiments.^[15]

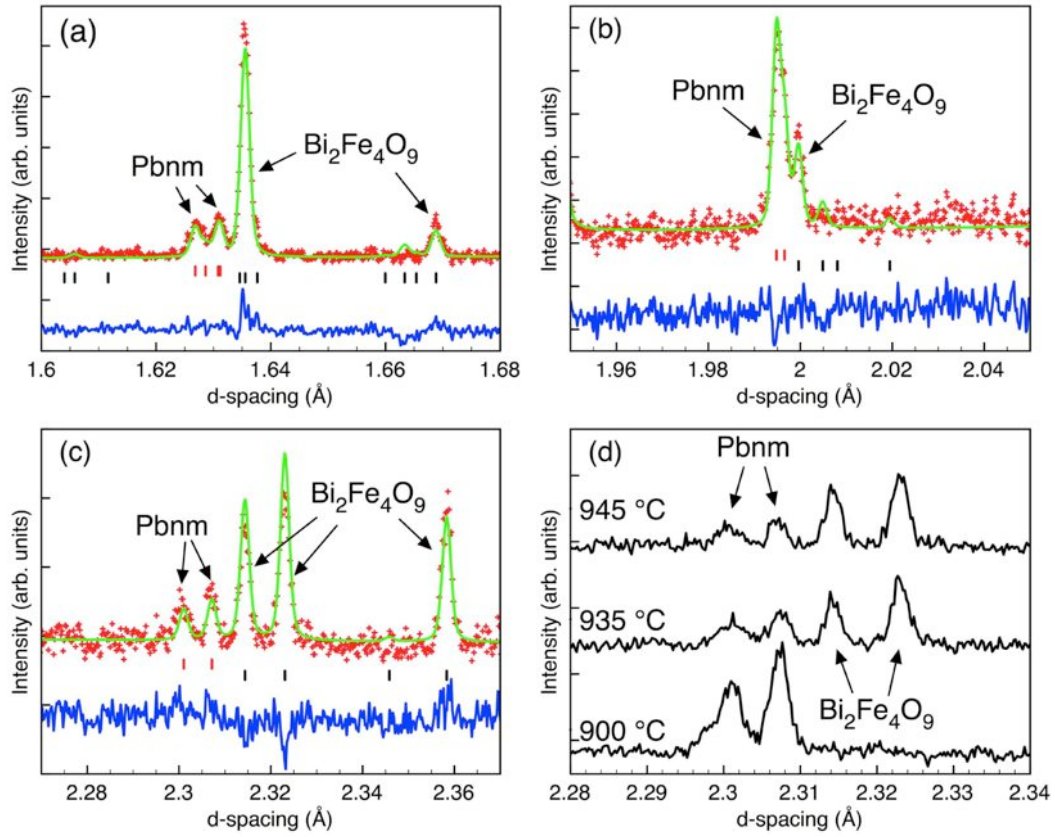


Figure 3: Expanded portions of the refinement profiles for data at 945 °C highlighting three different regions (a) to (c) clearly showing peak splitting which violate cubic and tetragonal symmetries and (d) showing that two distinct BiFeO₃ peaks which violate cubic and tetragonal symmetries remain through the insulator-metal transition. (Parts (a)-(c) colour online).

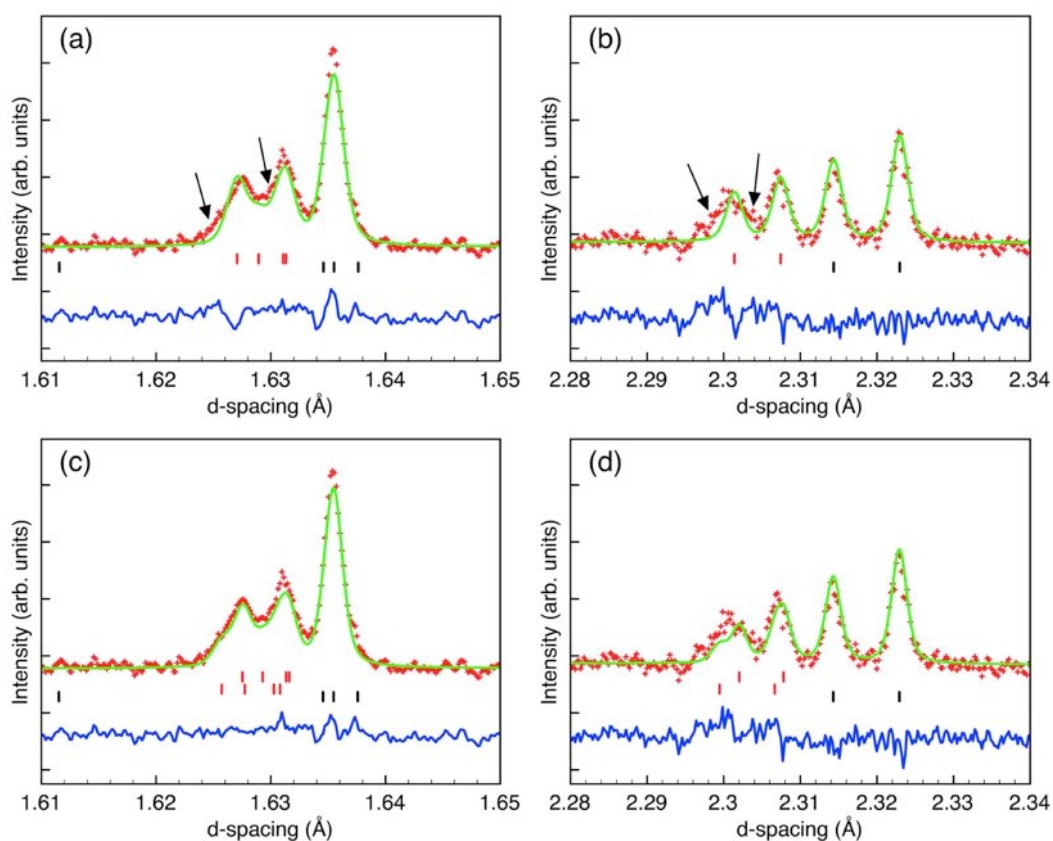


Figure 4: Expanded portions of the refinement profiles at 930 °C (a) and (b) fitted to a single Pbnm phase, clearly showing peak shoulders (marked by arrows) and the improved fit (c) and (d) achieved modelling two orthorhombic (Pbnm) phases with different lattice parameters (see table 2). (Colour online).

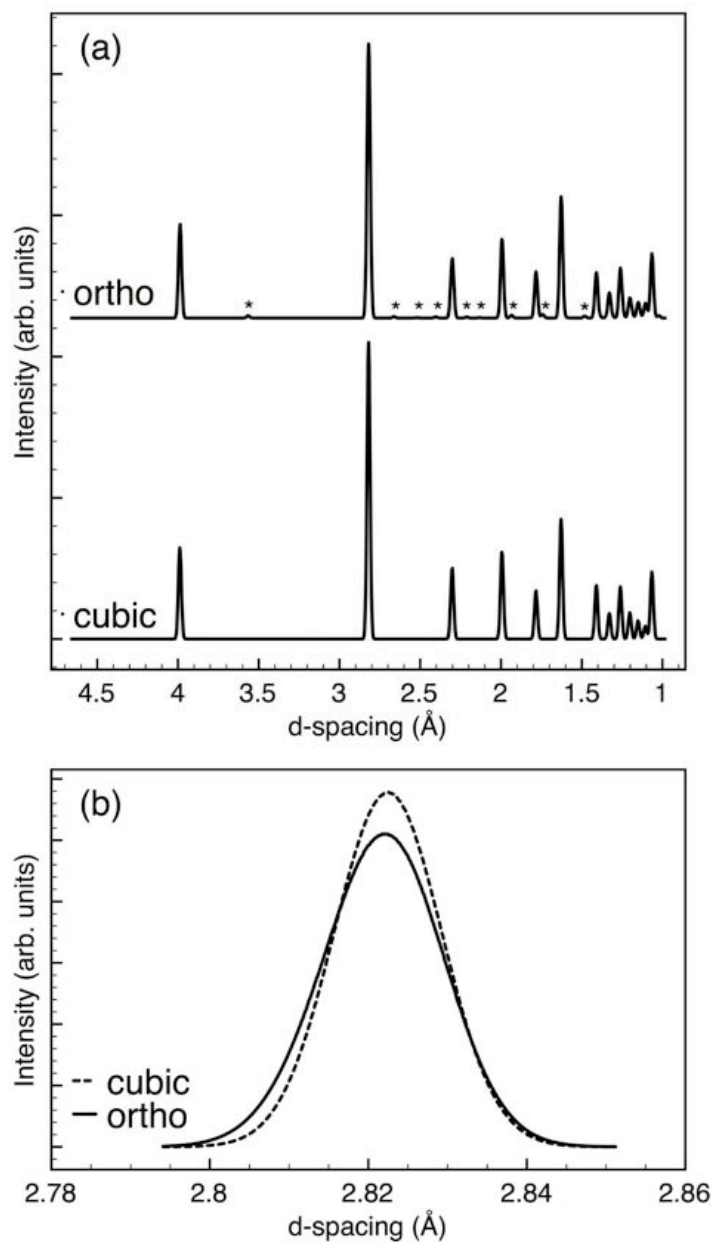


Figure 5: Simulation of the expected XRPD spectra (a) showing the differences between cubic (Pm-3m) and orthorhombic (Pbnm) symmetries emphasising the difficulties in resolving the weak superlattice reflections (marked *) associated with the orthorhombic symmetry and (b) expanded region indicating the similarities in the profiles of the cubic (110) and corresponding orthorhombic peaks with peak broadening as determined from data obtained at 950 °C (figure 6).

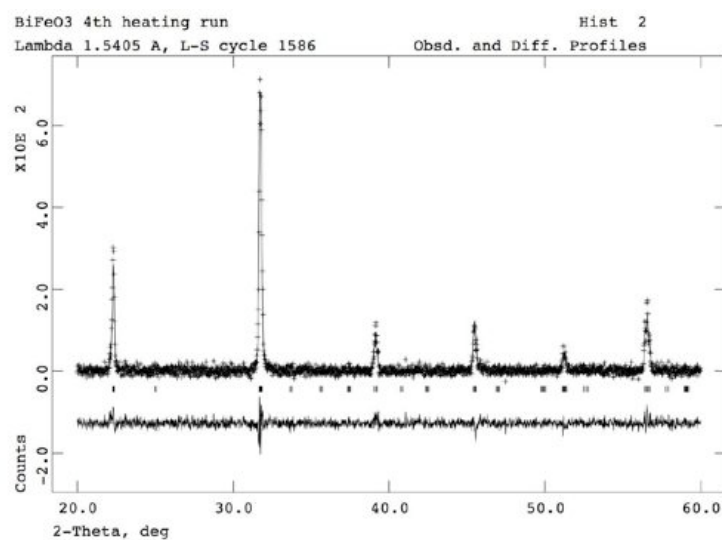


Figure 6: Refinement profiles of the XRPD data collected at 900 °C showing the observed (+), fitted (solid line) and difference curves (bottom) for BiFeO₃ (space group, Pbnm) as represented by the tick marks.

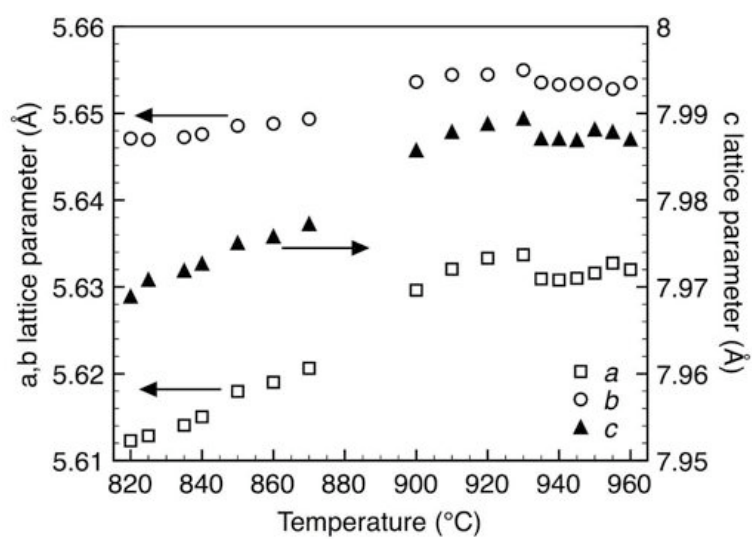


Figure 7: Lattice parameters as a function of temperature as extracted from powder neutron diffraction data. (Correlation between x-ray and neutron diffraction data is presented in supplementary information).

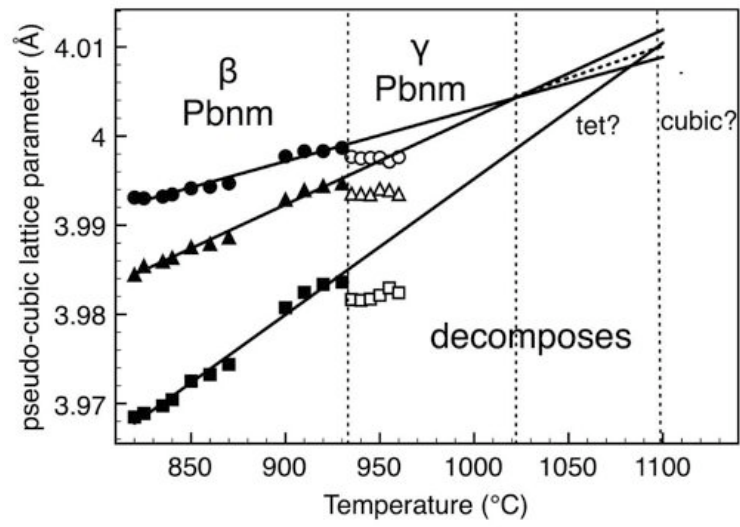


Figure 8: Extrapolation of pseudo-cubic cell parameters towards a unified value demonstrating the possible existence of an inaccessible cubic (or tetragonal) phase at temperatures beyond that of decomposition.

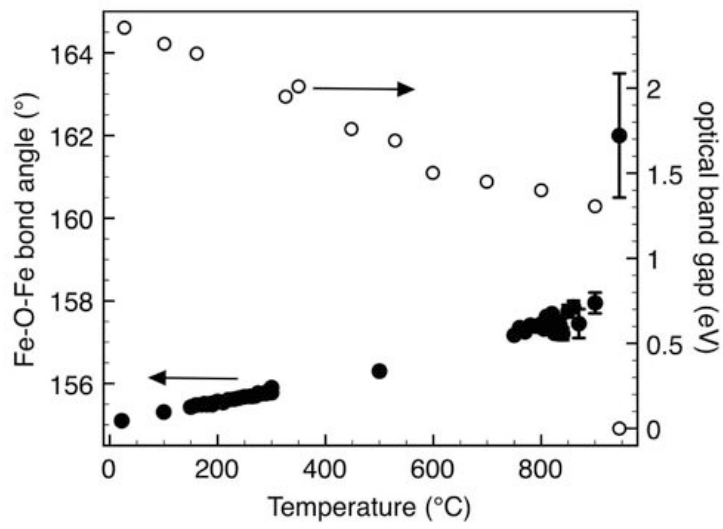


Figure 9: Relationship between Fe-O-Fe bond angle (additional data from Ref 15 and our unpublished work) and optical bandgap (data from Ref 12). Bond angle data for the β -phase is the average of the two observed angles.

Supplementary Information

Table S1: Parameters derived from Rietveld refinement of PND data as a function of temperature. Both β -BiFeO₃ and γ -BiFeO₃ were modelled in the orthorhombic space group Pbnm. Only lattice parameters were refined due to data quality with the exception of the 945 °C data as described in table 1 in the main text and marked (†) below.

T (°C)	χ^2	wRp (%)	Rp (%)	a (Å)	b (Å)	c (Å)	Cell Vol (Å ³)	% BiFeO ₃
910	0.976	7.81	7.87	5.6322(3)	5.6547(1)	7.9882(2)	254.41(2)	95
910	0.902	7.53	7.53	5.6319(3)	5.6542(1)	7.9875(2)	254.36(1)	93
920	0.901	7.50	7.46	5.6338(1)	5.6547(2)	7.9889(2)	254.51(1)	85
920	0.945	7.65	7.60	5.6328(2)	5.6543(2)	7.9886(2)	254.43(1)	78
930	0.942	7.69	7.65	5.6337(2)	5.6550(2)	7.9894(2)	254.53(1)	66
930	0.947	7.82	7.77	5.6317(2)	5.6539(2)	7.9880(2)	254.35(1)	56
930*	0.919	7.70	7.63	5.6335(2)	5.6547(2)	5.6528(3)	254.51(2)	39
				5.6264(3)	5.6528(3)	7.9828(5)	253.89(3)	17
935	0.923	7.74	7.78	5.6313(2)	5.6538(2)	7.9876(2)	254.31(1)	46
935	0.993	8.07	7.93	5.6306(2)	5.6533(2)	7.9866(2)	254.23(1)	41
940	0.971	8.09	7.89	5.6310(2)	5.6535(2)	7.9871(2)	254.27(1)	34
940	0.942	7.80	7.71	5.6306(2)	5.6532(2)	7.9870(2)	254.23(1)	33
945	1.153	8.49	8.06	5.6309(2)	5.6535(2)	7.9863(3)	254.24(2)	30
945 [†]	1.029	8.15	7.87	5.6311(2)	5.6538(2)	7.9885(3)	254.33(2)	27
950	0.918	7.88	7.69	5.6315(2)	5.6536(3)	7.9884(3)	254.34(2)	26
950	0.912	8.00	7.87	5.6317(3)	5.6533(3)	7.9879(3)	254.31(2)	22

* Refined with two orthorhombic phases

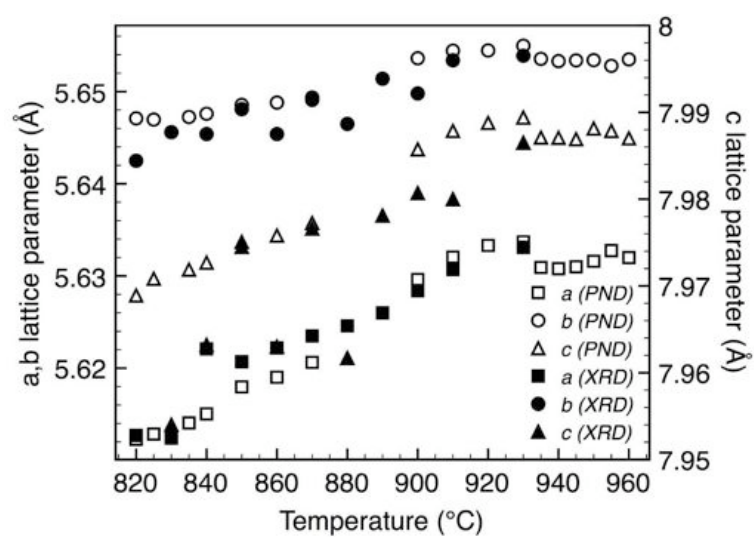


Figure S1. Comparison of lattice parameters obtained from data fitting of x-ray (XRD) and neutron (PND) diffraction data to the Pbnm space group.